ELSEVIER

Journal of Power Sources 52 (1994) 275–281

JOURNAL OF POWER SOURCES

# New manganese-substituted nickel hydroxides Part 2. Interstratification process upon ageing

L. Guerlou-Demourgues, C. Delmas *

*Laboratoire de Chimie du Solide du CNRS and Ecole Nationale Supérieure de Chimie et Physique de Bordeaux, Université Bordeaux I, 351 cours de la Libération, 33405 Talence Cedex, France*

Received 1 August 1994; accepted 10 September 1994

**Abstract**

The study of the ageing of the manganese-substituted nickel hydroxides with $\alpha$-structure in the KOH electrolytic medium of Ni/Cd batteries has given evidence of a new type of structure interstratification. This behaviour is due to spontaneous oxidation of the manganese ions, which are trivalent in the starting phases, to the tetravalent state in the aged materials. According to the infrared and chemical analysis results, the structure of the interstratified aged materials consists of a distribution of $\alpha$-, $\beta$(II)- and $\beta$(III)-interslab spaces directly related to fluctuations of the manganese distribution within the slabs.

*Keywords:* Nickel hydroxides; Manganese; Interstratification

## 1. Introduction

Previous works in our laboratory [1–4] have shown that partial substitution of cobalt or iron for nickel in nickel hydroxides leads, for substitution rates over 0.2, to the formation of $\alpha$-type phases stable in concentrated KOH solution (electrolytic medium of the Ni/Cd batteries). The structure cohesiveness in these phases results from strong electrostatic interactions between the trivalent M-substituting cations distributed within the $Ni_{1-y}M_yO_2$ slab and anions (generally $CO_3^{2-}$) inserted in the interslab space so as to perform the overall charge balance [2,3]. For small substitution amounts ($y < 0.2$), the number of inserted anions is insufficient to occupy all of the interslab spaces, which leads to anion segregation and therefore to interstratified materials [5]. The structure of the latter materials is still constituted of $Ni_{1-y}M_y(OH)_2$ slabs but with random stacking of $\alpha$-type interslab spaces (inserted with anions and water molecules) and $\beta$(II)-type ones (unoccupied).

This type of interstatified material has also been reported in the case of the homologous manganese system in the previous companion paper [6]. It is designated by I in Fig. 1, which gathers the various phases observed in the manganese system. A second type of interstratification has been evidenced for this system [6]. When aged for one month in KOH solution, the precipitated $\alpha$-materials that are obtained for $y$ manganese amounts $> 0.2$ tend to change spontaneously into interstratified materials. The latter ones have been designated by $I_A$ (the A index holds for 'aged') in Fig. 1 in order to avoid any confusion with the interstratified phases directly obtained by precipitation for $y < 0.2$ (I materials). Chemical characterizations and magnetic measurements have shown that the manganese ions, which are trivalent in the $\alpha$-phases, tend to be oxidized to $Mn^{4+}$ in the $I_A$-interstratified materials.

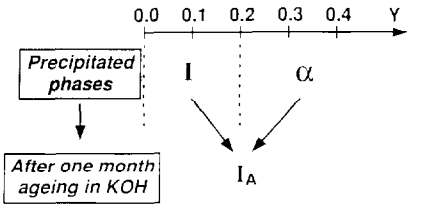


Fig. 1. Overview of the various phases obtained as a function of the manganese-substitution amount.

In the $\alpha$-type nickel hydroxides, and more generally in the related layered double hydroxides or in the mineral reevesite, about 0.5 $H_2O$ molecule per metal ion is present in the interslab space [7,8]. Taking into consideration that an $\alpha$-type interslab space contains one oxygen site per metal cation (triangular lattice), 0.5 oxygen site per metal cation is therefore left available

* Corresponding author.


*SSDI* 0378-7753(94)02024-W

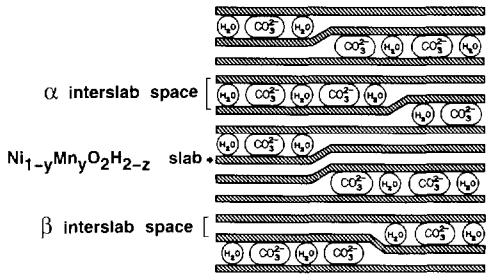


Fig. 2. Schematic representation of an interstratified structure constituted of $\alpha$- and $\beta$-type interslab spaces.

for anion insertion. Hence, 0.17 $CO_3^{2-}$ or 0.5 $OH^-$ anions can be theoretically at most intercalated as charge compensating species. It follows that, in the $I_A$-interstratified materials which contain $Mn^{4+}$ ions, the overall charge balance could be totally ensured by $CO_3^{2-}$ anions for $y$ manganese substitution amounts up to 0.17 or by $OH^-$ anions for $y$ values up to 0.25. Consequently, for higher manganese amounts, the charge compensation cannot be performed only by anionic insertion. This consideration leads one to assume the existence of proton deficiency in the slab. Hence, the interstratified structure of the $I_A$-materials may consist of $\alpha$- and $\beta$-type interslab spaces, but with $Ni_{1-y}Mn_yO_2H_{2-z}$-type slabs, as shown schematically in Fig. 2.

This hypothesis is investigated in the present paper and a mechanism for the interstratification process is proposed on the basis of infrared and chemical analyses data.

## 2. Results and discussion

As detailed in the previous companion paper [6], the starting manganese-substituted materials ($\alpha$ or I) have been prepared by precipitation of nickel and manganese salts by NaOH. The oxidation of the manganese ions into the trivalent state is performed with a 5 M $H_2O_2$ solution.

In the present paper, our attention will exclusively be focused on the series of interstratified materials obtained after ageing for a long period of time (one month) of the $\alpha$-phases in 5 M KOH medium.

It should be noticed that, while below $y=0.4$ pure $I_A$-interstratified phases are obtained, the $y=0.4$ composition leads in fact to a mixture constituted of an interstratified material ($I_A$-type) and of a $\gamma$-type nickel oxyhydroxide (exhibiting an intersheet distance close to 7 Å) [6]. This behaviour, which may originate from manganese composition fluctuations in the material, will be discussed in the following.

### 2.1. Chemical cycling from the $\alpha$- or $I_A$-hydroxides

Keeping in mind that the manganese-substituted nickel hydroxides are intended to be used as positive electrode materials in Ni/Cd cells, it is convenient to perform a chemical cycling in order to simulate the electrochemical behaviour. On account of the instability of the $\alpha$-manganese-substituted phases in 5 M KOH electrolytic medium (they transform into $I_A$-interstratified phases), both $\alpha$- and $I_A$-materials have been chemically cycled. As our original purpose consists in stabilizing the $\gamma/\alpha$-cycling, the chemical cycling has been essentially carried out for $y$ manganese substitution amounts equal to 0.2 or 0.3, which give rise to $\alpha$-phases.

#### 2.1.1. Preparation procedure

Two successive steps are involved in the chemical cycling from the $\alpha$- and $I_A$-phases [9].

(i) The first step consists in oxidizing the hydroxides: 1 g of $\alpha$- or $I_A$-material is introduced into 100 ml of oxidizing solution (4 M KOH, 0.8 M NaClO). The mixture is stirred for 15 h, the material is then washed, filtered and dried at 40 °C.

(ii) The second step consists in reducing the previously obtained oxyhydroxide. For this purpose, about 1 g of oxyhydroxide is set in suspension in 100 ml of distilled water, and then 50 ml of 0.5 M $H_2O_2$ solution are gradually dropped under stirring.

It should be noticed that, whereas oxygen peroxide was used to oxidize the $Mn^{2+}$ ions during the precipitation of the $\alpha$-phases, it acts as a reducing agent towards the metal cations in the nickel oxyhydroxide during the second step of the chemical cycling. The involved redox couple is therefore $O_2/H_2O_2$.

#### 2.1.2. X-ray diffraction study

The X-ray diffraction patterns of the various phases involved during the chemical cycling form an $\alpha$-($y=0.3$)phase are displayed in Fig. 3. Similar behaviours

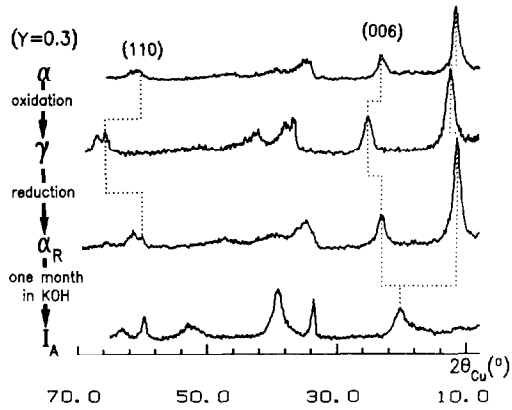


Fig. 3. X-ray diffraction patterns of the $\gamma$-, $\alpha_R$- and $I_A$-phases obtained by chemical cycling compared with that of the starting $\alpha$-hydroxide with $y=0.3$ composition.

are observed when the chemical cycling is performed from the materials with $y=0.2$ or $y=0.4$ composition.

The X-ray diffraction pattern of the material obtained after oxidation of the $\alpha$-phase (Fig. 3) is characteristic of a $\gamma$-phase. The latter crystallizes, like $\alpha$, in the rhombohedral system with $P3$ structural type. The decrease of the interslab distance during oxidation from 7.8 Å in the $\alpha$-phase down to 7 Å in the $\gamma$-one results from the modification of the interslab space composition: protons and carbonate ions are removed while alkali ions ($K^+$, $Na^+$ coming from the KOH–NaClO medium) are intercalated. The oxidation reaction is particularly well emphasized by the variation of the $a_{hex}$ parameter ($2d_{(110)}$), i.e., the metal–metal intraslab distance, which decreases from about 3.1 Å in the $\alpha$-phase down to about 2.8 Å in the $\gamma$-phase.

The formation of $\gamma$-phases by oxidation of $\alpha$-ones was commonly observed in the homologous cobalt system [2,10], whereas no complete chemical oxidation of the iron-substituted $\alpha$-phases into $\gamma$-ones was possible as a result of the very oxidizing character of these $\gamma$-materials [11].

The $\gamma$-type phases can also be obtained by oxidation of the $I_A$-interstratified phases resulting from the ageing of the freshly precipitated $\alpha$-materials. On the basis of the X-ray diffraction and chemical characterizations, the latter materials are quite identical to the $\gamma$-phases originating from the $\alpha$-phases.

As illustrated by the X-ray diffraction patterns in Fig. 3, reduction of a $\gamma$-oxyhydroxide leads to an $\alpha$-type phase that will be designated in the following by $\alpha_R$ (the R index holds for 'reduction'). Like the freshly precipitated $\alpha$-phases, the $\alpha_R$-phases are unstable in 5 M KOH solution; they transform into $I_A$-interstratified materials. This evolution is emphasized in Fig. 3 in the case of the $y=0.3$ composition.

A similar behaviour is observed when the complete cycling is performed from an $I_A$-material (arising from ageing in KOH of an $\alpha$-phase) as the starting phase. Nevertheless, in that case, the starting and final $I_A$-materials are identical on the basis of X-ray diffraction, infrared and chemical analysis characterizations. It follows that only the results concerning the $\alpha_R$-phases obtained by chemical cycling from $\alpha$-phases are presented hereafter.

### 2.1.3. Average cationic oxidation state in the $\gamma$- and $\alpha_R$-phases

The chemical analysis of the $\gamma$-phases has shown that the average cationic oxidation state is close to 3.5 whatever the manganese amount. It follows that the oxidation state is rather imposed by the structure than by the Ni/Mn ratio. This is a quite general behaviour observed in $\gamma$-nickel oxyhydroxides whatever the nature of the substituted cation [2,10,12]. Determination of the individual oxidation state of the nickel or manganese ions in the $\gamma$-phases seems to be very difficult. Nevertheless, the facility for the $Mn^{3+}$ ions in being spontaneously oxidized by air to $Mn^{4+}$ during ageing of the phases, described in Part 1, see Ref. [6], leads to assume the tetravalent state of manganese in the oxyhydroxide. This hypothesis has been confirmed by the magnetic study.

The average cationic oxidation states in the $\alpha_R$-phases, determined by iodometric tritration, are summarized in Table 1. The results obtained for the $\alpha$- and $I_A$-materials have been reported for comparison [6].

The values reported for the $\alpha_R$-phases suggest, as in the case of the $I_A$-materials, the presence of $(1-y)Ni^{2+}$ and $yMn^{4+}$ ions within the slab. The difference in manganese oxidation state between the freshly precipitated $\alpha$-phases (trivalent manganese) and the $\alpha_R$-phases (tetravalent manganese) results from the weakening of the oxidizing power of $H_2O_2$ in the precipitation alkaline medium. In other words, in alkaline medium, $H_2O_2$ is only slightly oxidizing towards $Mn^{2+}$ ions, which are therefore oxidized to the trivalent state, whereas $Ni^{2+}$ ions are not oxidized in these conditions. On the opposite, during the reduction step of the $\gamma$-phase, which is carried out in neutral pH conditions, $H_2O_2$ is able to reduce both tetravalent and trivalent nickel down to the divalent state while the manganese tetravalent state is maintained. This selective reduction of the nickel ions has already been observed in the iron or cobalt systems [3,13], except that in this case, the substituting ions were reduced down to the trivalent state.

## 2.2. Study of the interstratification process

### 2.2.1. Chemical analysis of the $\alpha$-, $I_A$- and $\alpha_R$-phases

On the basis of the weight percentages of the carbon, hydrogen, nickel and manganese elements determined by chemical analysis of the materials, the $CO_3/(Ni+Mn)$ and $H/(Ni+Mn)$ molar ratios, i.e., the numbers of $CO_3^{2-}$ ions and H element per metal ion have been calculated. Their evolutions with manganese concentration in the $\alpha$-, $\alpha_R$- and $I_A$-materials, are summarized in Table 2.

Table 1
Variation of the average cationic oxidation states in the $\alpha$-, $\alpha_R$- and $I_A$-phases vs. manganese concentration

| $y$ | Oxidation state $\pm 0.05$ | | |
|---|---|---|---|
| | $\alpha$ | $\alpha_R$ | $I_A$ |
| 0.2 | 2.33 | 2.46 | 2.42 |
| 0.3 | 2.36 | 2.58 | 2.62 |
| 0.4 | 2.46 | 2.79 | 2.77 [a] |

[a] $(I_A+\gamma)$: two-phase mixture.

Table 2
Variation of $y$ vs. of the $CO_3/(Ni+(Mn)$ and $H/(Ni+Mn)$ molar ratios in the $\alpha$-, $\alpha_R$- and $I_A$-phases [a]

| $y$ | $CO_3/(Ni+Mn)$ molar ratio | | | $H/(Ni+Mn)$ molar ratio | | |
|---|---|---|---|---|---|---|
| | Materials | | | Materials | | |
| | $\alpha$ | $\alpha_R$ | $I_A$ | $\alpha$ | $\alpha_R$ | $I_A$ |
| 0.2 | 0.13 | 0.18 | 0.06 | 3.38 | 2.80 | 2.40 |
| 0.3 | 0.14 | 0.15 | 0.03 | 2.94 | 2.68 | 2.17 |
| 0.4 | 0.11 | 0.12 | 0.06[a] | 3.25 | 2.24 | 2.11[a] |

[a] Note: it should be recalled that the ageing in KOH of the $\alpha$-phase with $y=0.4$ composition leads to a two-phase mixture constituted of a $\gamma$-oxyhydroxide and an $I_A$-type phase.

It should be noticed that the amount of sulfate ions is very small in the $\alpha$-phases (about 0.01 $SO_4^{2-}$ per metal atom for all $y$ values) and totally negligible in the $\alpha_R$- and $I_A$-phases ($<0.003$).

*2.2.1.1. The α-phases*

It is convenient to discuss these results on the basis of the idealized chemical formula $Ni_{1-y}Mn_y(OH)_2(CO_3)_{y/2}(H_2O)_{0.5}$, deduced on the analogy of the reevesite $Ni_{0.75}Fe_{0.25}(OH)_2(CO_3)_{0.125}(H_2O)_{0.5}$ [7].

For $y=0.4$, a slight decrease in the carbonate ions amount is noticed. As suggested in the introductive part of this chapter, the maximal amount of $CO_3^{2-}$ ions that can be theoretically intercalated (0.17) is in this case insufficient to ensure the compensation of the positive charge excess due to 0.4 $Mn^{3+}$ within the slab, so that $OH^-$ ions may replace some $CO_3^{2-}$ ones. Taking into account the $CO_3^{2-}$, $SO_4^{2-}$ and $H^+$ amounts determined by chemical analysis as well as the average cationic oxidation state (2.46), the following formula may be proposed:

$$\underbrace{Ni_{0.6}Mn_{0.4}(OH)_2}_{\text{slab}}\quad\underbrace{(CO_3)_{0.11}(SO_4)_{0.01}(OH)_{0.22}(H_2O)_{0.51}}_{\text{species inserted in the interslab space or adsorbed on the grain surface (mainly } H_2O)}$$

The presence of intercalated $OH^-$ ions has already been reported for the iron-substituted $\alpha$-phase with $y=0.4$ composition [3].

In addition, for the $\alpha$-phases the values of the $H/(Ni+Mn)$ ratio are generally larger than 3, which is the theoretical value deduced from the above-mentioned formula. This results from the presence of intercalated $OH^-$ ions and extra water molecules adsorbed on the grain surface.

*2.2.1.2. The $I_A$-phases*

In the $I_A$-interstratified materials, the strong drop of the $H/(Ni+Mn)$ ratio to values largely lower than 3 suggests the occurrence of proton deficiencies within the slab and the removal of $H_2O$ molecules from the interslab space. The latter behaviour, as well as the noticeable decrease of the $CO_3/(Ni+Mn)$ ratio with regard to that observed in the $\alpha$-phases, are consistent with the disappearance of some $\alpha$-type motives in favour of $\beta$-type ones and therefore with the structure interstratification.

The pronounced decrease of the $H/(Ni+Mn)$ ratio versus $y$ in the $I_A$-phases is fully in agreement with the simultaneous increase of the amount of proton deficiencies required to neutralize the positive charge brought by the $Mn^{4+}$ ions.

*2.2.1.3. The $\alpha_R$-phases*

The manganese oxidation state shifts from +3 in the $\alpha$-phases to +4 in the $\alpha_R$-phases. This modification, which implies an increase in the positive charge excess, is consistent with the evolution of the $CO_3/(Ni+Mn)$ and $H/(Ni+Mn)$ ratio values observed in comparison with the $\alpha$- and $\alpha_R$-phases for a given $y$ composition (Table 2). Indeed, the carbonate amount is higher and the H content is lower in the $\alpha_R$-phases than in the $\alpha$-ones in order to ensure the overall charge compensation.

In fact, the amount of the H element in the $\alpha_R$-phases is intermediate between the values corresponding to the $\alpha$- and $I_A$-phases. Hence, the $\alpha_R$phases may be considered as reaction intermediaries involved during transformation of the precipitated $\alpha$-phases (containing $Mn^{3+}$ ions) into $I_A$-interstratified materials (containing $Mn^{4+}$ ions). This point will be detailed in the general discussion.

*2.2.2. Infrared study*

*2.2.2.1. Comparison of the infrared spectra of the α-, $\alpha_R$- and $I_A$-materials*

The various steps of the structure interstratification are clearly illustrated by the evolution of the infrared spectra of the $\alpha$-, $\alpha_R$- and $I_A$-materials reported in Fig. 4 for the $y=0.3$ substitution amount. The infrared spectra of the $\alpha$- and $I_A$-materials have been discussed in detail in Part 1 of this study [6]. Nevertheless, several points have to be detailed.

The infrared spectra of the $\alpha$- and $\alpha_R$-phases (Fig. 4) exhibit strong similarities:

(i) The large bands around 3400 and 1650 $cm^{-1}$ are characteristic of the stretching and bending vibration modes of the water molecules intercalated in the interslab space or absorbed on the grain surface.

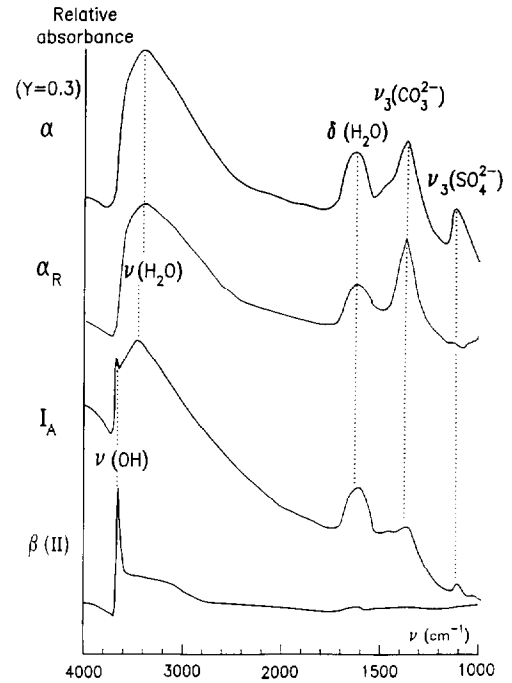


Fig. 4. Comparison of the infrared spectra of the $\alpha$-, $\alpha_R$-, $I_A$-phases ($y=0.3$) and $\beta$(II)-Ni(OH)$_2$ hydroxide.

(ii) The band at 1360 cm$^{-1}$ corresponds to the $\nu_3$ vibration mode of carbonate ions (in $D_{3h}$ symmetry), mainly inserted in the interslab space.

(iii) The vibration band at 1100 cm$^{-1}$ that is observed on the spectrum of the $\alpha$-phase characterizes the presence of a small amount of $SO_4^{2-}$ ions mainly absorbed on the grain surface, as previously discussed for the iron- or cobalt-substituted nickel hydroxides [12]. Those sulfate ions originate from the precipitation medium of the $\alpha$-phase (nickel and manganese sulfate solutions). They are removed during the chemical cycling steps, which accounts for the disappearance of the $\nu_3(SO_4^{2-})$ band on the infrared spectrum of the $\alpha_R$-phase.

As far as the $I_A$-phase is concerned, it should be recalled that it is characterized by the coexistence of both $\alpha$- and $\beta$-type interslab spaces:

(i) The appearance of the sharp $\nu$(OH) vibration band at 3650 cm$^{-1}$ shows that some hydroxyl groups of the slab are no longer hydrogen bonded with water molecules of the interslab space, as they are in the $\alpha$-type motives. This shows the formation of $\beta$(II)-Ni(OH)$_2$-type motives in the $I_A$-phase.

(ii) Nevertheless, the $\nu(H_2O)$, $\delta(H_2O)$ and $\nu_3(CO_3^{2-})$ vibration bands are characteristic of the species inserted in the $\alpha$-type interslab space [12]. Besides, comparison of the spectra of the $\alpha$- (or $\alpha_R$-) and $I_A$-materials shows a strong decrease in intensity of the $\nu_3(CO_3^{2-})$ band, which is consistent with the disappearance of some $\alpha$-type interslab spaces in favour of $\beta$-type ones when the structure interstratification occurs.

In the $I_A$-materials, as previously discussed on the basis of data of the chemical analyses, proton deficiencies must be present within the slabs in order to ensure the overall charge compensation. This behaviour suggests the presence of slabs with a strong $\beta$(III)-character. Moreover, the infrared spectroscopy results presented above show that both $\beta$(II)- and $\alpha$-type motives are simultaneously present in the $I_A$-phases. As a consequence, the three interslab types ($\beta$(II), $\beta$(III) and $\alpha$) must coexist in these materials. The interactions involved in the three motive types are schematized in Fig. 5. Whereas, in the $\beta$(II)-type domains, the OH groups are free, they are hydrogen bonded either with unprotonated oxygen atoms in the $\beta$(III)-type domains or with water molecules in the $\alpha$-type domains. These interactions result in the last two cases in the absence of the $\nu$(OH) vibration band [13,14]. Moreover, the distribution of the species in the interslab space and that of the $Mn^{4+}$ ions within the slab must be strongly correlated. As indicated in Fig. 5, the domains with high manganese content will be $\beta$(III)-type while those with very small manganese content will rather be $\beta$(II)-type, the intermediate manganese contents leading to $\alpha$-type domains.

*2.2.2.2. Evolution of the infrared spectra of the $I_A$-materials with y manganese concentration*

The evolution with manganese concentration of the infrared spectra of the $I_A$-interstratified phase is reported in Fig. 6. The decrease in intensity of the band assigned to the $\nu$(OH) vibration has to be pointed out. This behaviour indicates a decrease in $y$ of the 'free' hydroxyl groups amount, i.e., of the $\beta$(II)-type domain extent, probably in favour of $\beta$(III)-type domains. This evolution is indeed consistent with the increase in the amount of proton deficiencies required to perform the charge compensation when the $y$ tetravalent manganese concentration increases. As a matter of fact, a $y$ increase must promote the appearance of domains with high

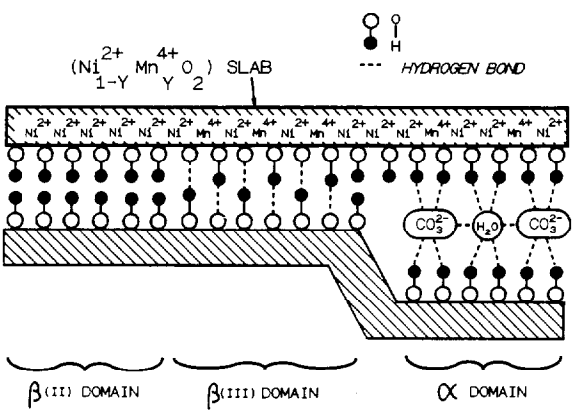


Fig. 5. Schematic representation of the various interslab space domains according to the manganese distribution within the slab.

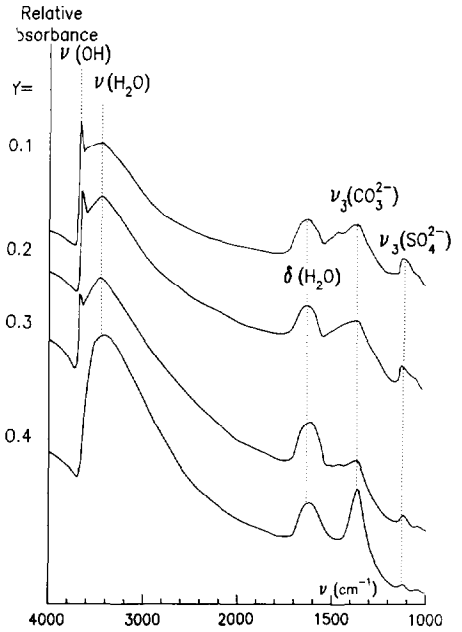


Fig. 6. Evolution of the infrared spectra of the $I_A$-interstratified materials as a function of the $y$ manganese amount.

manganese content, i.e., of $\beta$(III)-type domains, as shown schematically in Fig. 5.

*2.2.2.3. Special behaviour of the $y=0.4$ composition*

For the $y=0.4$ manganese concentration, the X-ray diffraction study shows that the ageing of the $\alpha$-phase in KOH leads to a phase mixture containing $I_A$- and $\gamma$-phases. As emphasized on the infrared spectrum by the absence of the $\nu$(OH) vibration band, no more $\beta$(II)-type domain is observed. This behaviour suggests that the structure of the $I_A$-phase is mainly constituted of $\alpha$- and $\beta$(III)-type interslab spaces. Fluctuations in the manganese composition within the material may account for the formation of this ($\gamma+I_A$)-mixture, the domains with the highest manganese content (strongly proton deficient) being likely to give rise to the $\gamma$-phase. The appearance of this phase is corroborated by the chemical analyses, which shows the increase of the $K^+/(Ni+Mn)$ ratio from 0.001 in the $\alpha$-phase up to 0.02 in the aged material.

## 2.3. General discussion

In order to confirm the general evolution suggested by the infrared study reported in Section 2.2.2., it is possible to estimate the distribution of the $\alpha$-, $\beta$(II)- and $\beta$(III)-domains for a material with given composition, on the basis of the X-ray diffraction pattern and of the data of the chemical analyses.

For instance, in the case of the $I_A$-phase with $y=0.2$, the starting data are as follows:

(i) the material contains 75% $\beta$-interslab spaces and 25% $\alpha$-ones (as deduced by the X-ray diffraction study previously reported), and

(ii) the $CO_3/(Ni+Mn)$ molar ratio is equal to 0.06 (Table 2).

Neglecting the absorbed species, the material formula can be therefore written as follows:

$$\underbrace{Ni_{0.8}Mn_{0.2}O_2H_z}_{\text{slab}}\ \underbrace{(CO_3)_{0.06}(H_2O)_t}_{\text{interslab space}}$$

where $z$ designates the number of H atoms linked to the oxygen atoms of the slabs and $t$ the number of $H_2O$ molecules inserted within the $\alpha$-planes. Taking into consideration the average cationic oxidation state (2.42) reported in Table 1, the overall charge compensation leads to $z=1.70$. Among these H atoms, 0.50 of them belong to the $Ni_{0.8}Mn_{0.2}(OH)_2$ slabs of the 0.25 $\alpha$-type planes. It follows that 1.20 H atoms are present in the $Ni_{0.8}Mn_{0.2}O_2H_w$ slabs of the 0.75 $\beta$-type planes where $w=1$ for $\beta$(III) or $w=2$ for $\beta$(II). Keeping in mind that one ideal $\beta$(II)-plane contains 2 H atoms per (Ni+Mn) atom while one $\beta$(III)-plane contains only one H atom, the numbers of $\beta$(II)- and $\beta$(III)-planes per metal atom ($r_{II}$ and $r_{III}$, respectively) are easily deduced from the following equation system:

$$r_{II}+r_{III}=0.75$$

$$2r_{II}+r_{III}=1.20$$

This leads to:

$$r_{II}=0.45$$

$$r_{III}=0.30$$

As a consequence, the structure of the $I_A$-($y=0.2$)phase is constituted of: 25% $\alpha$-type planes; 45% $\beta$(II)-planes and 30% $\beta$(III)-planes.

Calculations similar to those reported above for $y=0.2$ lead for the $I_A$-($y=0.3$)material to the following interslab space distribution: 25% $\alpha$-type planes; 13% $\beta$(II)-planes, and 62% $\beta$(III)-planes.

A mechanism for the interstratification process is proposed hereafter, on the basis of the overall results presented in this paper. Fig. 7 gives an overview of the chemical and structural modifications involved in such a process. From a general viewpoint, the electronic configuration of the $Mn^{3+}$ (HS) ions ($3d^4$) induces a Jahn–Teller effect, so that these ions are stabilized in a very distorted ($MnO_6$) octahedral site. In the freshly precipitated $\alpha$-phases, within the $Ni_{1-y}Mn_yO_2$ slabs, $Mn^{3+}$ ions are partially substituted for $Ni^{2+}$ (HS) ions ($3d^8$) which, as exhibiting a regular octahedral environment, prevent any cooperative distortion. As a consequence, the $Mn^{3+}$ ions are strongly destabilized. This entails a spontaneous oxidation of the $Mn^{3+}$ ions into the tetravalent state, during the ageing of the $\alpha$-phase

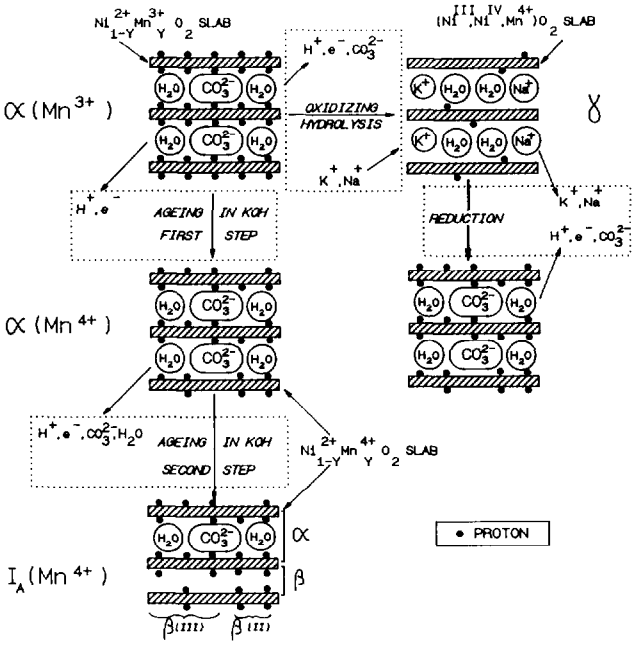


Fig. 7. Schematic representation of the various species exchanges involved in the interstratification process and in the chemical cycling from a manganese-substituted $\alpha$-phase.

in KOH medium, which must contribute to relax the structure.

This ageing of the freshly precipitated $\alpha$-($Mn^{3+}$)phases in KOH solution ($y \geqslant 0.2$) therefore leads in a first step to a partial slab deprotonation, resulting in the formation of a phase designated by $\alpha$-($Mn^{4+}$) in Fig. 7. This slab deprotonation is all the more likely as the enhanced covalency of the $Mn^{4+}$–O bond, antagonistic to the O–H one, must promote the proton lability. The $\alpha_R$-type phases, obtained by the chemical oxidation of the $\alpha$-phase into the $\gamma$-phase followed by a reduction, seem to be quite similar to this $\alpha$-($Mn^{4+}$)material.

In a second step, as a result of the electrostatic repulsion between the $CO_3^{2-}$ ions in the interslab space and the unprotonated oxygen ions of the slab, $CO_3^{2-}$ ions tend to be removed from the interslab space. This induces the collapse of the $\alpha$-type motives giving rise to $\beta$-ones on one hand, and the creation of new proton deficiencies so as to maintain the overall charge balance on the other hand.

## 3. Conclusions

The ageing of manganese-substituted $\alpha$-phases in KOH electrolytic medium leads to interstratified materials ($I_A$) which contain $Mn^{4+}$ ions. The overall results show that the interstratified structure of these materials is constituted of a random distribution of $\alpha$-type interslab spaces and of '$\beta$'-type ones with high proton vacancy content within the slabs. These '$\beta$'-type motives must be in fact considered as a mixture of $\beta$(II)- and $\beta$(III)-type domains as shown in Fig. 7.

## Acknowledgement

The authors are very grateful to C. Denage for her technical assistance.

## References

[1] C. Delmas, J.J. Braconnier, Y. Borthomieu and P. Hagenmuller, *Mater. Res. Bull., 22* (1987) 741.
[2] C. Faure, C. Delmas and P. Willmann, *J. Power Sources, 35* (1991) 263.
[3] L. Demourgues-Guerlou, J.J. Braconnier and C. Delmas, *J. Solid State Chem., 104* (1993) 359.
[4] L. Demourgues-Guerlou and C. Delmas, *J. Power Sources, 45* (1993) 281.
[5] Y. Borthomieu, L. Demourgues-Guerlou and C. Delmas, in J. Rouxel, M. Tournoux and R. Brec (eds.), *Proc. Int. Symp. Soft Chemistry Route to New Materials, Nantes, France, 6–10 Sept. 1993.*
[6] L. Guerlou-Demourgues, C. Denage and C. Delmas, *J. Power Sources, 52* (1994) 269–274.
[7] H.F.W. Taylor, *Mineral. Mag., 39* (1973) 377.
[8] W.T. Reichle, *Solid State Ionics, 22* (1986) 135.
[9] J.J. Braconnier, C. Delmas, C. Fouassier, M. Figlarz, B. Beaudoin and P. Hagenmuller, *Rev. Chim. Miner., 21* (1984) 496.
[10] C. Faure, C. Delmas, M. Fouassier and P. William, *J. Power Sources, 35* (1991) 249.
[11] L. Demourgues-Guerlou, L. Fournès and C. Delmas, *J. Solid State Chem.*, in press.
[12] C. Faure, Y. Borthomieu, C. Delmas and M. Fouassier, *J. Power Sources, 36* (1991) 113.
[13] F.P. Kober, *J. Electrochem. Soc., 112* (1965) 1064.
[14] M. Figlarz and S. Le Bihan, *C.R. Ac. Sci., 272* (1971) 580.